Syntheses and Properties of a Series of Cationic Water-Soluble Phthalocyanines

Hairong Li, Timothy J. Jensen, Frank R. Fronczek, and M. Graça H. Vicente*

Louisiana State University, Department of Chemistry, Baton Rouge, Louisiana 70803

Received June 29, 2007

A series of symmetrical cationic phthalocyanines (Pcs) with either Zn(II) or Si(IV) metal ions and two bulky axial ligands on the silicon complexes was synthesized in high yields. The photophysical (absorption, emission, fluorescence, and singlet oxygen quantum yields) and cellular (uptake, toxicity, and subcellular localization) properties of this series of Pcs were investigated. The Si(IV)−Pcs exist mainly as monomers in aqueous media and have higher fluorescent quantum yields in protic solvents (methanol and water) than the Zn(II)−Pcs. The presence of eight short PEG groups at the periphery of a Zn(II)−Pc significantly increases its solubility in protic solvents, but a centrally chelated silicon ion and associated bulky axial ligands were more efficient in preventing aggregation of the Pc macrocycles. The singlet oxygen quantum yields for this series of Pcs in DMSO are in the range 0.09–0.15. All Pcs were readily taken up by human HEp2 cells, and the extent of their accumulation within cells depends on their hydrophobic character. Intracellularly, all Pcs localized preferentially within the cell lysosomes. The Zn(II)−Pc **11** and Si(IV)−Pcs **12** and **14** were found to be the most phototoxic ($IC_{50} = 2.2$ μM at a 1 J cm^{-2} light dose) of this series of compounds.

Introduction

Photodynamic therapy (PDT)[a] is a binary modality for cancer treatment that uses a photosensitizer (PS) and visible light to produce reactive oxygen species which selectively destroy malignant cells.[1] PDT is currently used in several countries for the treatment of several types of cancer, including skin, mouth, esophageal, lung, and bladder tumors.[2–7] The selectivity of the PDT treatment depends upon both the tumor-targeting ability of the PS and the light used to activate it. An ideal PS should have minimal dark toxicity, high selectivity for tumors, rapid clearance from normal tissues, and a strong absorption peak within the "therapeutic window" (600–800 nm) for optimal light penetration through tissue.[8,9] Since the first approval of hematoporphyrin derivative (HpD) as a PS for PDT clinical applications, a large number of porphyrin derivatives have been synthesized and investigated for application in PDT; these include *meso*-tetraarylporphyrins, porphyrin dendrimers, core modified porphyrins, chlorins, bacteriochlorins, and Pcs.[10–13] From these studies, a number of second generation PSs have emerged. For example, tetra(meta-hydroxyphenyl)chlorin, 2-(1-hexyloxyethyl)-2-devinyl-pyropheophorbide a, and mono-L-aspartyl chlorin e_6 are currently being evaluated in PDT clinical trials. Pcs are particularly promising PSs for PDT because of their intense absorptions at ~680 nm (about 2 orders of magnitude larger in intensity than porphyrin long wavelength absorptions) and their ability for generating singlet oxygen.[1–4] However, Pcs are notorious for their strong tendency to aggregate in aqueous solutions,[14,15] which can significantly decrease their photosensitizing ability through self-quenching.[16] In order to decrease Pc aggregation and to increase their photodynamic activity, several hydrophilic and amphiphilic groups (e.g., carboxylates, sulfonates, phosphonates, PEGs)[17–20] and bulky axial ligands [e.g., $OSiMe_2(CH_2)_3NMe_2$ and $OCH(CH_2NMe_2)_2$][21–24] have been introduced at the macrocycle periphery and core, respectively.

Of particular interest are positively charged Pcs, since such molecules could potentially target highly vulnerable intracellular sites and cause effective DNA photodamage.[25,26] For example, it was reported that a series of cationic zinc pyridyloxy Pcs have higher photodynamic activity than purified HpD, the first FDA-approved PS for PDT, and that their biological efficacy could be modulated upon the introduction of alkyl chains of different length on the pyridyloxy groups.[27–29] Furthermore, positively charged Pcs have been successfully used for the photoinactivation of both Gram-negative and -positive bacteria.[30,31] On the other hand, Si(IV)−Pcs containing one or two bulky axial ligands usually show reduced aggregation, enhanced water-solubility, and high photodynamic efficacy. Recently, two glucosylated Si(IV)−Pcs were shown to have high phototoxicity toward human carcinoma HT29 and HepG2 cells[32] and a Si(IV)−Pc bearing two solketal axial substituents was found to be highly phototoxic to both 14C and B16F10 cell lines.[33] In our continuing investigation of new water-soluble and effective PDT sensitizers, we decided to combine, in a single macrocycle, peripheral cationic pyridyloxy groups and two bulky axial ligands on centrally chelated Si(IV) ions. Herein, we report the synthesis, photophysical evaluation, and in vitro investigations of a series of cationic 3-pyridiloxy Pcs bearing either a methyl or a short PEG chain on the pyridyl groups and Zn(II) or Si(IV) coordinating metals, with two large axial ligands on the silicon complexes. The properties of this new series of water-soluble Pcs are compared and discussed.

Experimental Section

1. Chemistry. All air and moisture sensitive reactions were performed under an argon atmosphere. All solvents and reagents were purchased from commercial sources, unless otherwise stated. Dry solvents excluding methanol were purified using a Braun solvent purification system. Dry methanol was obtained by redistillation after refluxing over calcium hydride for 5 h. Silica gel 60 (230 × 400 mesh, Sorbent Technologies) was used for column chromatography. Analytical thin-layer chromatography (TLC) was carried out using polyester backed TLC plates 254 (precoated, 200 μm) from Sorbent Technologies. NMR spectra were recorded on DPX-250 or ARX-300 Bruker or Varian Inova-500 spectrometers (250, 300, or 500 MHz for ^{1}H; 63, 75, or 125 MHz for ^{13}C). The chemical shifts are reported in δ ppm using the following deuterated solvents as internal references: CD_2Cl_2 5.32 (^{1}H), 53.8 ppm (^{13}C);

* To whom correspondence should be addressed. Phone: 225-578-7405. Fax: 225-578-3458 . E-mail: vicente@lsu.edu.

[a]Abbreviations: Pc, phthalocyanine; PS, photosensitizer; PDT, photodynamic therapy; PEG, polyethylene glycol; DMF, dimethylformamide; DMSO, dimethylsulfoxide; THF, tetrahydrofuran; DBU, 1,8-diazabicyclo[5.4.0]undec-7-ene; DPBF, 1,3-diphenylisobenzofuran; HEPES, 4-(2-hydroxyethyl)-1-piperazine ethane sulfonic acid: PBS, phosphate buffered saline; FBS, fetal bovine serum; ER, endoplasmic reticulum.

10.1021/jm070781f CCC: $40.75
Published on Web 01/12/2008

d-TFA 11.5 (^{1}H), 164.2 ppm (^{13}C); d-DMSO 2.49 (^{1}H), 39.5 ppm (^{13}C); d-THF 3.58 (^{1}H), 1.73 ppm (^{13}C); d-CH_3OH 4.78 (^{1}H), 49.0 ppm (^{13}C); d-DMF 8.01 (^{1}H), 162.7 ppm (^{13}C); CD_3CN 1.93 (^{1}H), 118.2 ppm (^{13}C); D_2O 4.63 ppm (^{1}H). Electronic absorption spectra were measured on a Perkin-Elmer Lambda 35 UV–vis spectrometer. IR spectra were recorded with a Bruker Tensor 27 spectrophotometer. Mass spectra were obtained on either a Bruker ProFlex III MALDI-TOF mass spectrometer using α-cyano-4-hydroxycinnamic acid or dithranol as the matrix or an Applied Biosystems QSTAR XL quadrupole TOF MS for ESI. Elemental analyses were performed on a Thermo Finnigan Flash 1112 CHN elemental analyzer. Melting points were measured on a Fisher-Johns apparatus.

4,5-Bis(pyridin-3-yloxy)phthalonitrile (2). 4,5-Dichlorophthalonitrile (1.0 g, 5.0 mmol) and 3-hydroxypyridine (2.2 g, 23.1 mmol) were dissolved in 15 mL of dry DMF at 80 °C under argon. Potassium carbonate (4.5 g, 32.6 mmol) was added to the reaction solution in 8 portions every 5 min. The reaction solution was heated for 3 h, then cooled to room temperature, and poured into 100 mL of ice–water. After filtration under vacuum, the crude product was purified by column chromatography on neutral alumina using methanol/dichloromethane 1:50 for elution. The title compound (1.37 g) was obtained as a pale white solid in 86% yield. ^{1}H NMR (CD_2Cl_2): δ 8.53 – 8.51 (m, 2H, Py-H), 8.42 (s, 2H, Py-H), 7.42–7.41 (m, 4H, Py-H), 7.31 (s, 2H, Ar-H). ^{13}C NMR (CD_2Cl_2): δ 151.53, 147.46, 142.19, 127.18, 125.24, 123.67 (Ar-C, Py-C), 115.21 (CN), 112.19 (Ar-C). FTIR (solid): 2236.8 (CN), 1211.3 (C−O) cm^{-1}. MS (MALDI-TOF) *m/z* 315.31 [M + H] $^+$, calcd. for $C_{18}H_{11}N_4O_2$ 315.09. Anal. calcd. for $C_{18}H_{10}N_4O_2$: C 68.79, H 3.21, N 17.83. Found: C 68.58, H 3.33, N 17.78.

Crystal data for **2**: Colorless, $C_{18}H_{10}N_4O_2$, $M_r = 314.3$, monoclinic space group *C*2/*c*, $a = 24.573(3)$, $b = 9.417(2)$, $c = 16.076(3)$ Å, $\beta = 128.21(2)°$, $V = 2923.0(12)$ Å^3, $Z = 8$, $\rho_{calcd} = 1.428$ g cm^{-3}, Mo Kα radiation ($\lambda = 0.71073$ Å; $\mu = 0.098$ mm^{-1}), $T =$ 110 K, 32 427 data points by Nonius KappaCCD, $R = 0.057$ (3531 with $F^2 > 2\sigma$), $R_w = 0.149$ (all F^2) for 5539 unique data points having $\theta < 33.1°$ and 217 refined parameters, CCDC 652076. Crystals were grown by slow evaporation of dichloromethane.

Triethylene Glycol Iodide. Compound $CH_3(OCH_2CH_2)_3I$ was synthesized from the corresponding tosylate $CH_3(OCH_2CH_2)_3Ts$, which was prepared according to Schultz's procedure[34] in 88% yield. The following data is for triethylene glycol tosylate $CH_3(OCH_2CH_2)_3Ts$: ^{1}H NMR (CD_2Cl_2): δ 7.78 (d, $J = 8.3$ Hz, 2H, Ar-H), 7.37 (d, $J = 8.3$ Hz, 2H, Ar-H), 4.12 (t, $J = 4.5$ Hz, 2H, OCH_2), 3.64 (t, $J = 4.5$ Hz, 2H, OCH_2), 3.53 (s, 6H, OCH_2), 3.49 (t, $J = 1.6$ Hz, 2H, OCH_2), 3.32 (s, 3H, OCH_3), 2.44 (s, 3H, Ar-CH_3). ^{13}C NMR (CD_2Cl_2): δ 145.44, 133.24, 130.22, 128.21 (Ar-C), 72.22, 71.01, 70.77, 70.72, 69.84, 68.92 (OCH_2), 58.95 (OCH_3), 21.72 (Ar-CH_3). MS (ESI) *m/z* 319.12 [M + H]$^+$, 320.13 [M + 2H]$^+$, 336.15 [M + H_2O]$^+$, 341.10 [M + Na]$^+$, calcd. for $C_{14}H_{23}O_6S$ 319.12, $C_{14}H_{24}O_6S$ 320.13, $C_{14}H_{24}O_7S$ 336.12, $C_{14}H_{22}NaO_6S$ 341.10. To a solution of this compound (10 g, 0.031 mol) in 80 mL of dry acetone was added NaI (9.9 g, 0.062 mol), and the reaction was refluxed for 20 h. After cooling to room temperature, the solution was filtered under vacuum and washed with acetone. The filtrate was collected and concentrated. The residue was dissolved in 100 mL of dichloromethane, washed successively with 1 N sodium thiosulfate solution and brine, and dried over anhydrous sodium sulfate. The solvent was removed under vacuum and the product was obtained as a light yellow liquid (8.5 g) in 98% yield. ^{1}H NMR (CD_2Cl_2): δ 3.73 (t, $J = 6.8$ Hz, 2H, OCH_2), 3.64–3.56 (m, 6H, OCH_2), 3.52–3.48 (m, 2H, OCH_2), 3.33 (s, 3H, OCH_3), 3.27 (t, $J = 6.8$ Hz, 2H, OCH_2). ^{13}C NMR ($CDCl_3$): δ 77.42, 77.00, 76.58, 71.77, 70.42, 70.03 (OCH_2), 58.85 (OCH_3). MS (ESI) *m/z* 275.01 [M + H]$^+$, 292.04 [M + H_2O]$^+$, calcd. for $C_7H_{16}IO_3$ 275.01, $C_7H_{17}IO_4$ 292.02.

Bis(pyridine-3-yloxy)diiminoisoindoline (3). Phthalonitrile **2** (2 g, 6.4 mmol) and sodium methoxide (0.5 g, 9.3 mmol) were dissolved in 100 mL of freshly distilled methanol. Ammonia gas was bubbled into the solution for 50 min at room temperature. The solution was then heated to 65 °C and refluxed under a slow stream of ammonia gas for 5 h. The solvent was removed under reduced pressure. Water (150 mL) was added to the concentrated residue to precipitate the product. The product was filtered and washed thoroughly with water to afford light green crystals of the title compound (1.9 g) in 91% yield; mp 122–124 °C. ^{1}H NMR ($CDCl_3$): δ 8.32–8.16 (m, 3H, NH), 7.42–7.12 (m, 10H, Ar-H, Py-H). ^{13}C NMR (d-DMSO): δ 152.97, 148.32, 144.85, 140.13, 124.95, 124.71, 113.63 (Ar-C, Py-C). FTIR (solid): 3036.73, 2963.08, 1667.2 (CN), 1213.2 (CO) cm^{-1}. MS (MALDI-TOF) *m/z* 332.20 [M + H]$^+$, 354.14 [M + Na]$^+$, calcd. for $C_{18}H_{14}N_5O_2$ 332.11, $C_{18}H_{13}N_5O_2Na$ 354.10.

ZnPc (4). Phthalonitrile **2** (0.4 g, 1.27 mmol) and zinc acetate dihydrate (0.1 g, 0.45 mmol) were mixed and heated at 80 °C in 15 mL of dry pentanol. After adding a few drops of DBU, the temperature was raised to 140 °C. The mixture was heated overnight and then concentrated under reduced pressure. The crude product was washed three times successively with dichloromethane, acetone, and cold methanol. The title product was obtained as a dark green solid (0.37 g) in 88% yield; mp > 250 °C. UV–vis (DMSO): λ_{max} (log ε) 678 (4.08) nm. ^{1}H NMR (d-TFA): δ 9.60 (s, 8H, Ar-H), 9.00 (s, 8H, Py-H), 8.81 (br, 8H, Py-H), 8.62 (br, 8H, Py-H), 8.29 (br, 8H, Py-H). ^{13}C NMR (d-TFA): δ 159.07, 156.10, 151.27, 139.77, 137.94, 137.23, 134.47, 131.88, 121.24 (Ar-C, Py-C). MS (MALDI-TOF) *m/z* 1320.78 [M$^+$], calcd. for $C_{72}H_{40}N_{16}O_8Zn$ 1320.25.

ZnPc (10). Pc **4** (0.2 g, 0.15 mmol) and 25 mL of CH_3I were stirred at 40 °C, and the reaction was followed by ^{1}H NMR. After 1 day, methyl iodide was removed under reduced pressure. The crude product was washed with acetone to yield the title compound as a dark green solid (0.35 g) in 96% yield; mp > 250 °C. UV–vis (DMSO): λ_{max} (log ε) 677 (4.84), 611 (4.21), 359 (4.48) nm. ^{1}H NMR (D_2O): δ 9.16 (s, 8H, Ar-H), 9.00 (s, 8H, Py-H), 8.56 (d, $J = 6.1$ Hz, 8H, Py-H), 8.48 (d, $J = 8.4$ Hz, 8H, Py-H), 8.00–8.04 (m, 8H, Py-H), 4.32 (s, 24H, CH_3). ^{13}C NMR (D_2O): δ 157.24, 151.70, 147.57, 142.07, 137.20, 136.06, 134.66, 130.38, 117.26 (Ar-C, Py-C), 50.00 (CH_3). MS (MALDI-TOF) *m/z* 1320.48 [M − 8I − 8CH_3]$^+$, 1335.43 [M − 8I − 7CH_3]$^+$, calcd. for $C_{72}H_{40}N_{16}O_8Zn$ 1320.25, $C_{73}H_{43}N_{16}O_8Zn$ 1335.27.

ZnPc (11). Pc **4** (0.02 g, 0.015 mmol) and $CH_3(OCH_2CH_2)_3I$ (1.5g, 5.5 mmol) were heated to 70 °C in a sealed 10 mL thick-walled tube for 6 days. The product was isolated from the reaction solution by centrifugation and washed twice with acetone and twice with dichloromethane. The crude product was purified on a Sephadex LH-20 column using methanol for elution. The product was vaccuum-dried at 30 °C for 2 days to afford the title compound as a dark green solid (56 mg) in 92% yield; mp 173–175 °C. UV–vis (DMF): λ_{max} (log ε) 675 (4.74), 609 (4.10), 354 (4.36) nm. UV–vis (H_2O):λ_{max} (log ε) 674 (4.56), 611 (3.94), 351 (4.27). ^{1}H NMR (d-DMF): δ 9.69 (s, 8H, Ar-H), 9.60 (s, 8H, Py-H), 9.21 (d, $J = 5.3$ Hz, 8H, Py-H), 8.88 (d, $J = 7.6$ Hz, 8H, Py-H), 8.48–8.42 (m, 8H, Py-H), 5.12 (br, 16H, OCH_2), 4.16 (br, 16H, OCH_2), 3.72 (br, 16H, OCH_2), 3.57–3.44 (m, 48H, OCH_2), 3.26 (s, 24H, OCH_3). ^{13}C NMR (d-DMF): δ 157.24, 153.86, 147.70, 142.12, 137.98, 136.65, 134.73, 129.97, 117.57 (Ar-C, Py-C), 72.34, 70.81, 70.66, 69.63, 62.21 (OCH_2), 58.70 (OCH_3). MS (MALDI-TOF) *m/z* 1320.60 [M − 8PEG]$^+$, 1467.04 [M − 7PEG]$^+$, 1613.94 [M − 6PEG]$^+$, 1762.01 [M − 5PEG]$^+$, calcd. for $C_{72}H_{40}N_{16}O_8Zn$ 1320.25, $C_{79}H_{55}N_{16}O_{11}Zn$ 1467.35, $C_{86}H_{70}N_{16}O_{14}Zn$ 1614.46, $C_{93}H_{85}N_{16}O_{17}Zn$ 1761.56. HRMS-ESI *m/z* 549.9806 [M − 6I − H]$^{5+}$, 575.5675 [M − 5I]$^{5+}$, 751.9363 [M − 4I]$^{4+}$, 1044.5473 [M − 3I]$^{3+}$, calcd. for $[C_{128}H_{159}I_2N_{16}O_{32}Zn]^{5+}$ 549.9737, $[C_{128}H_{160}I_3N_{16}O_{32}Zn]^{5+}$ 575.5562, $[C_{128}H_{160}I_4N_{16}O_{32}Zn]^{4+}$ 751.9437, $[C_{128}H_{160}I_5N_{16}O_{32}Zn]^{3+}$ 1043.8633.

SiPc (5). Dry diiminoisoindoline **3** (0.5 g, 1.5 mmol) was added to 5 mL of freshly redistilled quinoline. The reaction solution was stirred under argon for 10 min ,and then, silicon tetrachloride (0.5 mL, 2.2 mmol) was added dropwise to the solution. The temperature was raised to 220 °C and maintained for 1 h. The solution was cooled to room temperature, and the solid was filtered under vacuum and washed successively with water, methanol, and acetone. The title compound was obtained as a dark green solid (0.5 g) in 98% yield; mp > 250 °C. UV–vis (DMSO): λ_{max} (log ε) 677 (3.83) nm.

^{1}H NMR (d-TFA): δ 9.66 (br, 8H, Ar-H), 8.98 (br, 8H, Py-H), 8.73 (br, 8H, Py-H), 8.58 (br, 8H, Py-H), 8.21 (br, 8H, Py-H). ^{13}C NMR (d-TFA): δ 158.95, 152.09, 151.43, 139.324, 137.64, 136.40, 134.08, 131.48, 120.53 (Ar-C, Py-C). MS (MALDI-TOF) *m/z* 1319.82 $[M - Cl]^+$, calcd. for $C_{72}H_{40}ClN_{16}O_8Si$ 1319.27.

SiPc (6). A mixture of Pc **5** (0.45 g, 0.33 mmol) and sodium methoxide (1.5 g, 27 mmol) in 60 mL of water/ethanol (5:1) was heated to reflux for 5 h. The solvent was removed under reduced pressure, and the product was isolated by precipitation upon addition of 10 mL of water. The slurry solid was filtered and washed thoroughly with water. The final product was dried under vacuum at 40 °C for 2 days to afford the title compound as a dark green solid (0.35 g) in 81% yield; mp > 250 °C. UV–vis (DMSO): λ_{max} (log ε) 677 (4.11), 609 (3.64), 364 (3.94) nm. ^{1}H NMR (d-TFA): δ 9.72 (br, 8H, Ar-H), 9.03 (br, 8H, Py-H), 8.81 (br, 8H, Py-H), 8.64 (br, 8H, Py-H), 8.29 (br, 8H, Py-H). ^{13}C NMR (d-TFA): δ 159.11, 152.24, 151.58, 139.46, 137.78, 136.55, 134.20, 131.61, 120.67 (Ar-C, Py-C). FTIR (solid): 3382.3 (O−H), 1209.5 (C−O), 844.6 (Si−O) cm^{-1}. MS (MALDI-TOF) *m/z* 1301.81 $[M - OH]^+$, 1318.63 $[M]^+$, calcd. for $C_{72}H_{41}N_{16}O_9Si$ 1301.30, $C_{72}H_{42}N_{16}O_{10}Si$ 1318.30.

SiPc (7). Pc **6** (0.17 g, 0.125 mmol) was dissolved in 10 mL of dry pyridine at 115 °C under an argon atmosphere. Chlorotripropylsilane (0.7 mL, 3.2 mmol) was added dropwise to the reaction solution via syringe. After 8 h, another portion of chlorotripropylsilane (0.5 mL, 2.2 mmol) was added. The reaction solution was refluxed for another 9 h. The solvent was evaporated to dryness, and 10 mL of pentane was added. After sonication for 5 min, the crude product was obtained by centrifugation. The solid was further purified using a short silica column and THF for elution. The title compound was dried under vacuum at 40 °C and obtained as a dark green solid (0.11 g, 52%); mp > 250 °C. UV–vis (CH_2Cl_2): λ_{max} (log ε) 674 (5.34), 644 (4.54), 607 (4.60), 360 (4.92) nm. ^{1}H NMR (d-THF): δ 9.30 (s, 8H, Ar-H), 8.58 (d, J = 2.7 Hz, 8H, Py-H), 8.46 (dd, J = 1.0, 4.5 Hz, 8H, Py-H), 7.63–7.59 (m, 8H, Py-H), 7.45–7.41 (q, 8H, Py-H), −0.15 (t, J = 7.2 Hz, 18H, CH_3), −0.99 to −1.07 (m, 12H, CH_2), −2.29 to −2.34 (m, 12H, CH_2). ^{13}C NMR (d-THF): δ 154.75, 151.75, 149.04, 146.15, 141.46, 133.91, 125.48, 125.09, 116.40 (Ar-C, Py-C), 17.84, 16.42, 15.87 ($CH_2CH_2CH_3$). MS (MALDI-TOF) *m/z* 1457.88 $[M - OSi(C_3H_7)_3]^+$, calcd. for $C_{81}H_{61}N_{16}O_9Si_2$ 1457.44.

SiPc (12). Pc **7** (20 mg, 0.01 mmol) and CH_3I (7 mL) reacted as described above for Pc **10**, and the title compound was obtained as a green solid (27 mg, 95%); mp > 250 °C. UV–vis (H_2O): λ_{max} (log ε) 674 (5.03), 644 (4.31), 607 (4.35), 356 (4.68) nm. ^{1}H NMR (d-DMF): δ 10.10 (s, 8H, Ar-H), 9.67 (s, 8H, Py-H), 9.21 (d, 8H, J = 5.6 Hz, Py-H), 8.81 (d, 8H, J = 8.3 Hz, Py-H), 8.48–8.43 (m, 8H, Py-H), 4.71 (s, 24H, N−CH_3), −0.12 (t, 18H, J = 7.0 Hz, CH_3), −0.99 to −1.08 (m, 12H, CH_2), −2.31 to −2.37 (m, 12H, CH_2). ^{13}C NMR (d-DMF): δ 156.57, 150.05, 148.78, 142.99, 138.67, 135.09, 134.51, 130.06, 117.89 (Ar-C, Py-C), 49.56 (N-CH_3), 17.80, 16.07, 15.57 ($CH_2CH_2CH_3$). MS (MALDI-TOF) *m/z* 1644.87 $[M - 7CH_3 - 8I]^+$, 1456.46 $[M - OSi(C_3H_7)_3 - 8CH_3 - 8I]^+$, calcd. for $C_{91}H_{85}N_{16}O_{10}Si_3$ 1645.59, $C_{81}H_{61}N_{16}O_9Si_2$ 1457.44. HRMS-ESI *m/z* 795.1072 $[M - 3I]^{3+}$, 564.8538 $[M - 4I]^{4+}$, 532.6256 $[M - 5I - H]^{4+}$, 525.8209 $[M - 5I - (CH_3)_2 + H]^{4+}$, calcd. for $[C_{98}H_{106}I_5N_{16}O_{10}Si_3]^{3+}$ 795.0936, $[C_{98}H_{106}I_4N_{16}O_{10}Si_3]^{4+}$ 564.9740, $[C_{98}H_{105}I_3N_{16}O_{10}Si_3]^{4+}$ 532.6161, $[C_{96}H_{101}I_3N_{16}O_{10}Si_3]^{4+}$ 525.9824.

SiPc (8). Pc **6** (0.12 g, 0.088 mmol) and chlorotriisopropylsilane (0.4 mL, 1.8 mmol) reacted as described above for Pc **7** and the title compound was obtained as a dark green solid (94 mg, 64%); mp > 250 °C. UV–vis (CH_2Cl_2): λ_{max} (log ε) 677 (5.13), 646 (4.21), 609 (4.28), 359 (4.63) nm. ^{1}H NMR (d-DMF): δ 9.43 (s, 8H, Ar-H), 8.68 (s, 8H, Py-H), 8.57 (d, J = 4.4 Hz, 8H, Py-H), 7.84 (d, J = 8.4 Hz, 8H, Py-H), 7.64–7.59 (m, 8H, Py-H), −1.06 (d, J = 8.0 Hz, 36H, CH_3), −1.94 to −2.01 (m, 6H, CH). ^{13}C NMR (d-DMF): δ 154.36, 151.52, 148.90, 146.18, 141.22, 133.22, 126.15, 125.68, 116.01(Ar-C, Py-C), 16.11, 11.42 ($CH(CH_3)_2$). MS (MALDI-TOF) *m/z* 1631.23 $[M + H]^+$, 1457.42 $[M - OSi(C_3H_7)_3]^+$, calcd. for $C_{90}H_{83}N_{16}O_{10}Si_3$ 1631.58, $C_{81}H_{61}N_{16}O_9Si_2$ 1457.43.

SiPc (13). Pc **8** (35 mg, 0.02 mmol) and CH_3I (8 mL) reacted as described above for Pc **10**, and the title compound was obtained as a green solid (28 mg, 96%); mp > 250 °C. UV–vis (H_2O): λ_{max} (log ε) 677 (4.84), 648 (4.05), 610 (4.07), 356 (4.45) nm. ^{1}H NMR (d-DMF): δ 9.99 (s, 8H, Ar-H), 9.70 (s, 8H, Py-H), 9.22 (d, 8H, J = 5.5 Hz, Py-H), 8.88 (d, 8H, J = 7.4 Hz, Py-H), 8.48–8.46 (m, 8H, Py-H), 4.73 (s, 24H, N-CH_3), −1.07 (d, 36H, J = 7.4 Hz, CH_3), −1.99 to −2.06 (m, 6H, CH). ^{13}C NMR (d-DMF): δ 156.30, 149.94, 148.96, 142.92, 138.75, 135.08, 134.49, 130.02, 117.56 (Ar-C, Py-C), 49.49 (N−CH_3), 16.24, 11.33 ($CH(CH_3)_2$). MS (MALDI-TOF) *m/z* 1457.69 $[M - 8MeI - OSi(C_3H_7)_3]^+$, 1472.70 $[M - 7MeI - OSi(C_3H_7)_3]^+$, 1630.80 $[M - 8MeI]^+$, 1645.82 $[M - 7MeI]^+$, calcd. for $C_{81}H_{61}N_{16}O_9Si_2$ 1457.44, $C_{82}H_{64}N_{16}O_9Si_2$ 1472.46, $C_{90}H_{82}N_{16}O_{10}Si_3$ 1630.57, $C_{91}H_{85}N_{16}O_{10}Si_3$ 1645.59. HRMS-ESI *m/z* 795.4410 $[M - 3I]^{3+}$, 752.8038 $[M - 4I - H]^{3+}$, 564.6037 $[M - 4I]^{4+}$, 532.6259 $[M - 5I - H]^{4+}$, calcd. for $[C_{98}H_{106}I_5N_{16}O_{10}Si_3]^{3+}$ 795.6001, $[C_{98}H_{105}I_4N_{16}O_{10}Si_3]^{3+}$ 752.8038, $[C_{98}H_{106}I_4N_{16}O_{10}Si_3]^{4+}$ 564.5941, $[C_{98}H_{105}I_3N_{16}O_{10}Si_3]^{4+}$ 532.6161.

SiPc (9). Pc **6** (0.2 g, 0.15 mmol) and tert-butyldiphenylchlorosilane (0.8 mL, 3.0 mmol) reacted as described above for Pc **7** and the title compound was obtained as a dark green solid (99 mg, 37%); mp 185–187 °C. UV–vis (DMF):λ_{max} (log ε) 680 (5.09), 650 (4.29), 612 (4.36), 363 (4.59) nm. ^{1}H NMR (d-DMF): δ 9.19 (s, 8H, Ar-H), 8.75 (d, J = 2.6 Hz, 8H, Py-H), 8.60 (d, J = 4.5 Hz, 8H, Py-H), 7.92–7.90 (m, 8H, Py-H), 7.70–7.66 (m, 8H, Py-H), 6.99 (t, J = 7.3 Hz, 4H, Ar-H), 6.57 (t, J = 7.4 Hz, 8H, Ar-H), 4.91 (d, J = 7.1 Hz, 8H, Ar-H), −1.22 (s, 18H, $C(CH_3)_3$). ^{13}C NMR (d-DMF): δ 154.44, 151.27, 148.62, 146.13, 141.19, 133.79, 133.30, 133.21, 128.94, 126.94, 126.39, 125.78, 115.95 (Ar-C, Py-C), 24.99, 17.00 ($C(CH_3)_3$). MS (MALDI-TOF) *m/z* 1794.37 $[M^+]$, 1539.26 $[M - (OSiPh_2{}^tBu)]^+$, calcd for $C_{104}H_{78}N_{16}O_{10}Si_3$ 1794.54, $C_{88}H_{59}N_{16}O_9Si_2$ 1539.42.

SiPc (14). Pc **9** (20 mg, 0.01 mmol) and CH_3I (4 mL) reacted as described above for Pc **10**, and the title compound was obtained as a green solid (29 mg, 91%); mp 217–219 °C. UV–vis (H_2O): λ_{max} (log ε) 679 (4.81), 649 (3.96), 612 (4.01), 352 (4.29) nm. ^{1}H NMR (d-DMF): δ 9.79 (s, 8H, Ar-H), 9.71 (s, 8H, Py-H), 9.25 (d, J = 5.3 Hz, 8H, Py-H), 8.88 (d, J = 7.8 Hz, 8H, Py-H), 8.57–8.54 (m, 8H, Py-H), 7.04 (t, J = 7.3 Hz, 4H, Ar-H), 6.68 (t, J = 7.4 Hz, 8H, Ar-H), 4.89 (d, J = 7.0 Hz, 8H, Ar-H), 4.76 (s, 24H, N−CH_3), −1.24 (s, 18H, $C(CH_3)_3$). ^{13}C NMR (d-DMF): δ 156.47, 149.87, 148.76, 143.06, 138.95, 135.06, 134.24, 133.70, 133.05, 130.17, 129.32, 127.36, 117.61 (Ar-C, Py-C), 49.61 (N−CH_3), 25.24, 17.04 ($C(CH_3)_3$). MS (MALDI-TOF) *m/z* 1810.95 $[M - 7MeI - I + H]^+$, calcd. for $C_{105}H_{82}N_{16}O_{10}Si_3$ 1810.57. HRMS-ESI *m/z* 850.0984 $[M - (OSiPh_2{}^tBu) - I + 2H]^{3+}$, 606.0964 $[M - (OSiPh_2{}^tBu) - 2I + 2H]^{4+}$, 573.6194 $[M - (OSiPh_2{}^tBu) - 3I + H]^{4+}$, 541.6409 $[M - (OSiPh_2{}^tBu) - 4I]^{4+}$, calcd. for $[C_{96}H_{85}I_7N_{16}O_9Si_2]^{3+}$ 849.9846, $[C_{98}H_{85}I_6N_{16}O_9Si_2]^{4+}$ 606.1078, $[C_{96}H_{84}I_5N_{16}O_9Si_2]^{4+}$ 573.7842, $[C_{96}H_{83}I_4N_{16}O_9Si_2]^{4+}$ 541.8062.

SiPc (15). Pc **9** (45 mg, 0.025mmol) and $CH_3(OCH_2CH_2)_3I$ (2.2 g, 8.2 mmol) reacted as described above for Pc **11**, and the title compound was obtained as a dark green solid (94 mg, 94%); mp 82–84 °C. UV–vis (H_2O): λ_{max} (log ε) 678 (4.76), 649 (3.90), 610 (3.96), 353 (4.25) nm. ^{1}H NMR (CD_3CN): δ 9.58 (s, 8H, Ar-H), 9.43 (s, 8H, Py-H), 8.97 (d, J = 5.3 Hz, 8H, Py-H), 8.63 (d, J = 7.7 Hz, 8H, Py-H), 8.29 (t, J = 7.6 Hz, 8H, Py-H), 6.98 (t, J = 7.3 Hz, 4H, Ar-H), 6.57 (t, J = 7.3 Hz, 8H, Ar-H), 5.02 (br, 16H, OCH_2), 4.84 (d, J = 7.1 Hz, 8H, Ar-H), 4.14 (br, 16H, OCH_2), 3.70 (br, 16H, OCH_2), 3.55–3.47 (m, 48H, OCH_2), 3.28 (s, 24H, OCH_3), −1.26 (s, 18H, $C(CH_3)_3$). ^{13}C NMR (CD_3CN): δ 156.50, 149.97, 148.87, 142.63, 138.42, 136.02, 134.40, 133.96, 133.15, 130.39, 129.55, 127.50, 117.49 (Ar-C, Py-C), 72.48, 71.16, 70.88, 70.79, 69.38, 62.73 (OCH_2), 59.01 (OCH_3), 25.37, 17.20 ($C(CH_3)_3$). MS (MALDI-TOF) *m/z* 3985.42 $[M - H]^+$, 3603.91 $[M - OSiPh_2{}^tBu - I - H]^+$, 3476.98 $[M - OSiPh_2{}^tBu - 2I - H]^+$, 3348.09 $[M - OSiPh_2{}^tBu - 3I - 2H]^+$, 3221.20 $[M - OSiPh_2{}^tBu - 4I - 2H]^+$, calcd. for $C_{160}H_{197}I_8N_{16}O_{34}Si_3$ 3985.58, $C_{144}H_{178}I_7N_{16}O_{33}Si_2$ 3603.56, $C_{144}H_{178}I_6N_{16}O_{33}Si_2$ 3476.66, $C_{144}H_{177}I_5N_{16}O_{33}Si_2$ 3348.74, $C_{144}H_{177}I_4N_{16}O_{33}Si_2$ 3221.84. HRMS-ESI *m/z* 1202.3092 $[M - (OSiPh_2{}^tBu) - I + 2H]^{3+}$, 870.0024 [M

$-(OSiPh_2{}^tBu) - 2I + 2H]^{4+}$, 670.6225 $[M - (OSiPh_2{}^tBu) - 3I + 2H]^{5+}$, 645.2429 $[M - (OSiPh_2{}^tBu) - 4I + H]^{5+}$, calcd. for $[C_{144}H_{181}I_7N_{16}O_{33}Si_2]^{3+}$ 1202.1943, $[C_{144}H_{181}I_6N_{16}O_{33}Si_2]^{4+}$ 869.9196, $[C_{141}H_{181}I_5N_{16}O_{33}Si_2]^{5+}$ 670.5548, $[C_{144}H_{180}I_4N_{16}O_{33}Si_2]^{5+}$ 645.3780.

2. Photophysical Studies. All absorption spectra were measured on a Perkin-Elmer Lambda 35 UV–vis spectrometer with 10 mm path length quartz cuvettes. Emission spectra were obtained on a Fluorolog 3 spectrofluorimeter. Pure solvents were used as reference solutions. All solvents were either ACS spectrophotometric or HPLC grade. Sodium phosphate dibasic was purchased from EMD. Milli-Q water (resistance 18 MΩ) was prepared in-house. The phosphate buffer solutions were prepared by dissolving 1.43 g anhydrous sodium phosphate dibasic in 100 mL water followed by pH adjustment with concentrated hydrochloride or sodium hydroxide solution using a Thermo Orion Model 410 pH meter. Stock solutions (10 mM DMSO) of all Pcs were prepared. All dilutions were prepared by spiking 0.2–2 μL of the corresponding DMSO stock solutions into 1 mL of each solvent. The optical densities of the solutions used for the emission studies were between 0.04 and 0.05 at the excitation wavelength (610 nm) to eliminate inner filter effects. All the measurements were performed within 3 h of solution preparation.

Fluorescent quantum yields were calculated using a secondary standard method.[35] Methylene blue, a dye with excitation/emission wavelengths similar to Pcs, was used as the reference. The following equation

$$Q = Q_R \frac{I}{I_R} \frac{OD_R}{OD} \frac{n^2}{{n_R}^2}$$

was applied to calculate the quantum yield of the Pcs. In this equation, the fluorescence intensities of the analyte (I) and standard (I_R), optical densities of the analyte (OD) and standard (OD_R), and the refractive indexes of the analyte solvent (n) and standard solvent (n_R) are incorporated, in addition to Q_R, the quantum yield of the reference standard (0.03 for methylene blue).[36,37]

Singlet oxygen quantum yields were obtained in DMSO at room temperature, using ZnPc ($\Phi_\Delta = 0.67$) as reference and 1,3-diphenylisobenzofuran (DPBF) as scavenger, according to the procedure previously described.[38] The DPBF absorption decay was followed at 417 nm. The singlet oxygen quantum yields were determined with an accuracy of about 10%.

3. Partition Coefficients. The partition coefficients were measured at room temperature by adding 0.15 mL of Pc stock solution in DMSO to a 2 mL volumetric tube containing 1.0 mL of HEPES buffer (50 mM, pH 7.4) and 1.0 mL of octanol.[39] After vortexing for 1 min, the phases were separated by centrifugation. An aliquot of 0.15 mL from each layer was diluted with 1 mL of methanol and the absorbance was read on a Perkin-Elmer Lambda 35 UV–vis spectrometer with 10 mm path length quartz cuvettes.

4. Cell Culture. Human carcinoma HEp2 cells were maintained in a 50:50 mixture of DMEM:AMEM (Invitrogen) supplemented with 5% FBS (Invitrogen) and Primocin antibiotic (Invivogen). The cells were subcultured twice weekly to maintain subconfluent stocks.

4.1. Time-Dependent Cellular Uptake. The HEp2 cells were plated at 7500 cells per well in a Costar 96-well plate and allowed to grow for 48 h. Pc stock solutions were prepared at 10 mM in DMSO and diluted to give 20 μM in medium (a 2X stock). This was then further diluted into the wells of the 96-well plate to give a final concentration of 10 μM with a maximum DMSO concentration of 1%. Uptake was allowed to continue for 0, 1, 2, 4, 8, and 25 h. The uptake was terminated by removing the loading medium and washing the wells with PBS. The Pc concentration was measured using intrinsic fluorescence as measured with a BMG FLUOstar plate reader equipped with a 355 nm excitation and a 680 nm emission filter. The cell numbers were measured using a CyQuant Cell proliferation assay (Invitrogen) as per manufactures instructions.

4.2. Dark Cytotoxicity. The HEp2 cells were plated as described above for the uptake experiment. The Pc was diluted into medium to give a 100 μM concentration. 2-Fold serial dilutions were then prepared to 3.125 μM, and the cells were incubated overnight. Cell toxicity was measured using Promega's CellTiter Blue Viability Assay kit as per manufacturer's instructions, with untreated cells considered 100% viable and cells treated with 0.2% saponin as 0% viable.

4.3. Phototoxicity. The cells were prepared as described above with Pc concentration range 0.3125 to 10 μM. After loading overnight, the medium was replaced with medium containing 50 mM HEPES pH 7.2. The cells were exposed to a 100 W halogen lamp filtered through a 610 nm long pass filter to provide approximately 1 J cm^{-2} light dose. The cells were kept cool by filtering the IR radiation through 10 mm of water and placing the culture plate on an aluminum block in an ice–water bath, which acted as a heat sink. After exposure to light, the plate was incubated overnight. Cell toxicity was then measured as described above.

4.4. Microscopy. The cells were plated on Laboratory Tek II chamber slides (Nunc) and allowed to grow for 48 h. The cells were then exposed to 10 μM Pc overnight. Organelle tracers were obtained from Invitrogen and used at the following concentrations: LysoSensor Green (to visualize lysosomes and acidic compartments) 50 nM, MitoTracker Green (to visualize mitochondria) 250 nM, ER Tracker (to visualize the ER) 100 nM, and BODIPY FL C_5 ceramide (to visualize the Golgi complex) 1 μM. Images were acquired using a Zeiss Axiovert 200 M inverted fluorescent microscope equipped with an AxioCam MRm CCD camera. Pc fluorescence was imaged using standard Texas Red filters, and organelle tracers were imaged with standard FITC filters (Chroma Technologies).

Results and Discussion

1. Synthesis and Characterization. The water-soluble octapyridyloxy-Pcs **10**−**15** were synthesized as shown in Scheme 1, via quaternization of the corresponding Zn(II) or Si(IV) complexes. The dipyridyloxy-phthalonitrile **2** was prepared in 86% yield from commercially available 4,5-dichlorophthalonitrile **1** and 3-hydroxypyridine, as it has been previously reported by Wöhrle and co-workers.[40] The X-ray structure of this key intermediate is shown in Figure 1. One of the pyridine rings is disordered by 2-fold rotation, such that N4 and C17 superimpose. The other pyridine appears to be ordered. The two OPy groups are oriented differently with respect to the phthalonitrile, with torsion angles −59.8(2)° about C1−O1 and −7.0(2)° about C2−O2.

The macrocyclization of phthalonitrile **2** was accomplished under mild conditions, upon heating in dry 1-pentanol in the presence of zinc acetate and a catalytic amount of DBU, to give Zn(II)−Pc **4** in an improved 88% yield from that previously reported.[28,40] The neutral octapyridyloxy-Pc **4** is poorly soluble in most common organic solvents, but it is soluble in TFA. Alkylation of the pyridyl groups using either methyl iodide or $CH_3(OCH_2CH_2)_3I$ afforded the octa-cationic Zn(II)−Pcs **10** and **11** in 96 and 92% yields, respectively. Although highly soluble in DMSO and partially soluble in water, Pcs **10** and **11** aggregate in aqueous solutions, as indicated by the broadening of their Q bands and fluorescence quenching (vide infra).

Since eight alkylated pyridyl groups at the periphery of the Zn−Pc macrocycle still do not prevent its aggregation in aqueous solutions, we prepared a series of octapyridyloxy Si(IV)−Pcs bearing two bulky axial ligands. Phthalonitrile **2** was converted to the diiminoisoindoline **3** in 91% yield by reaction with ammonia gas (Scheme 1). Diiminoisoindoline **3** and an excess of silicon tetrachloride were heated to 220 °C in freshly distilled quinoline for 1 h giving Si(IV)−Pc dichloride **5** in 98% yield. The dihydroxylation of Pc **5** to give Pc **6** was accomplished using sodium methoxide in ethanol/water. The presence of the OH groups in Pc **6** was confirmed by FT-IR, which shows a broad peak at 3382.3 cm^{-1} (O−H) and a sharp

Scheme 1. Synthetic Route to Metallo-phthalocyanines 10−15

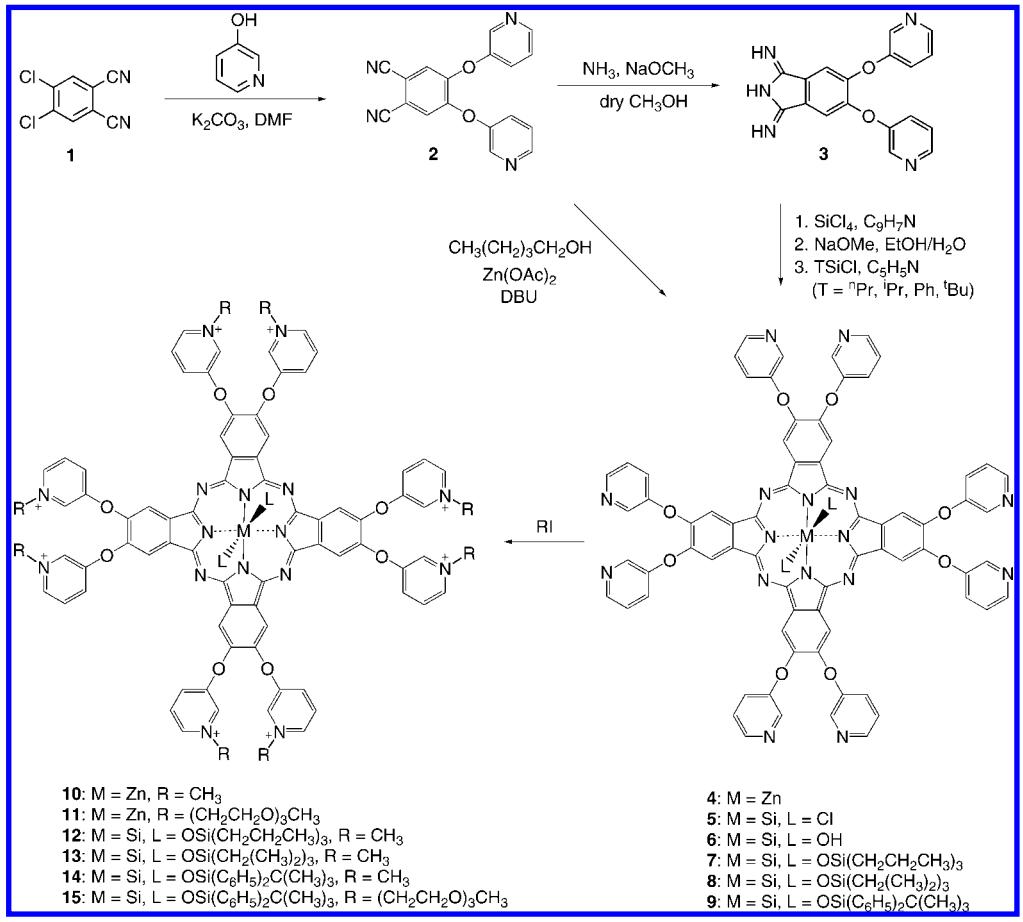

peak at 844.6 cm^{-1} (Si−O). Pcs **7**−**9** were obtained by reacting Pc **6** with a large excess of the corresponding alkylchlorosilane in dry pyridine, at 115 °C under an argon atmosphere. The excess silane reagent was washed out with pentane, and Pcs **7**−**9** were purified by column chromatography on silica gel, using THF for elution. The octapyridyloxy Si(IV)−Pcs **7**−**9** show high solubility in polar organic solvents, such as in DMF, THF, DMSO, methanol, and acetonitrile. The ^{1}H NMR spectra of **7**−**9** in either deuterated THF or DMF characteristically show the Pc macrocycle protons in the downfield region at >9 ppm, the pyridyl protons between 8 and 9 ppm, the aliphatic protons on the axial ligands significantly upfield shifted below 0 ppm, and the axial ligand aromatic protons below 7 ppm. The MALDI-TOF MS spectra of Pcs **5**−**9** all show the base peak corresponding to the cleavage of one axial ligand, as it is often observed for this type of compound (e.g., see ref 41). Alkylation of Si(IV)−Pcs **7**−**9** gave the corresponding octa-cationic derivatives **12**−**15** in yields higher than 90%. All cationic Si(IV)−Pcs were also characterized by NMR, MS, UV–vis, and fluorescence spectroscopy (vide infra) and are highly soluble in protic solvents such as methanol and water. All Pcs were >99% pure, as determined by HPLC (see Table S1 and Figures S1−S5 in the Supporting Information).

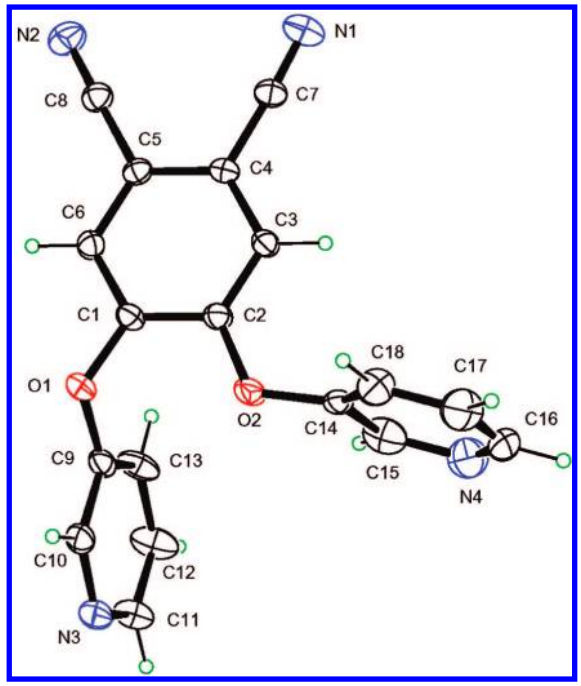

Figure 1. Molecular structure of phthalonitrile **2**, with 50% ellipsoids. Only one orientation of the disordered pyridine is shown.

2. Photophysical Studies. The spectral properties of Pcs **10**–**15** in DMSO, methanol, and water at different pH values are summarized in Table 1. Additional concentration- and time-dependent absorption and emission spectra in phosphate buffer at pH 7.4 and spectral data obtained in DMF and acetonitrile are shown in Tables S3 and S4 and in Figures S6–S21 in the Supporting Information. The absorption and emission properties of this series of phthalocyanines depend significantly on the solvent used and the solution pH. Both the nature of the *N*-pyridyl group (methyl vs triethylene glycol) and the centrally chelated metal and associated axial ligands affect the photophysical properties of the Pc macrocycles. The Si(IV)−Pcs bearing two bulky axial ligands show significantly higher

Table 1. Spectral Properties of Phthalocyanines 10−15 in Different Media[a]

media (pH)	10	11	12	13	14	15
DMSO						
abs	360, 611, 677	356, 611, 677	360, 608, 676	360, 610, 678	359, 612, 681	359, 612, 680
em	682	682	679	681	684	683
SS	5	5	3	3	3	3
QY	0.0614	0.0692	0.0518	0.0763	0.0361	0.0670
MeOH						
abs	349, 670	351, 607, 671	359, 603, 670	358, 606, 672	355, 607, 675	356, 608, 675
em	674	675	671	674	677	677
SS	4	4	1	2	2	2
QY	0.0394	0.0546	0.0958	0.1146	0.0748	0.0987
Aqueous (6.0)						
abs	346, 632, 667	351, 675	357, 608, 674	356, 610, 677	353, 612, 680	353, 611, 678
em	678	680	677	680	683	681
SS	11	5	3	3	3	3
QY	0.0032	0.0368	0.0839	0.0495	0.0449	0.0495
Aqueous (7.0)						
abs	346, 632, 667	350, 676	357, 608, 674	356, 610, 677	353, 612, 680	353, 611, 678
em	679	680	677	680	682	681
SS	12	4	3	3	2	3
QY	0.0038	0.0350	0.0732	0.0455	0.0566	0.0594
Aqueous (8.0)						
abs	347, 632, 668	352, 676	357, 608, 674	357, 610, 677	352, 612, 680	353, 611, 678
em	679	680	677	680	682	681
SS	11	4	3	3	2	3
QY	0.0033	0.0309	0.0756	0.0452	0.0604	0.0469

[a] abs, absorption maxima (nm); em, emission maxima (nm); SS, Stokes shift (nm); QY, quantum yield.

fluorescence quantum yields than the Zn(II)−Pcs, in all solvents studied. Among the Si(IV)−Pcs, Pc **12** bearing two flexible tri(*n*-propyl)siloxy axial groups has the highest fluorescence quantum yield in aqueous media at all pH values investigated (5.0. 6.0, 7.0, 7.4, and 8.0), whereas Pc **13** bearing two tri(isopropyl)siloxy axial groups, the most hydrophobic of the Si(IV)−Pcs synthesized (vide infra), has the highest quantum yield in organic solvents (DMSO and methanol). The neutral Si(IV)−Pcs **7**−**9** also showed high fluorescence quantum yields in organic solutions (see Table S4 of the Supporting Information). The fluorescence quantum yields of Pcs **10**−**15** in aqueous media were found to generally decrease with the pH, being the largest at pH 5.0 as we have previously observed.[42] The cationic Pcs bearing triethylene glycol chains on the pyridyloxy groups showed higher fluorescence quantum yields in organic solvents than the corresponding methylated Pcs, although in aqueous media similar values were observed (Table 1).

In DMSO, all Pcs show strong absorption and emission bands at ∼677 and 681 nm, respectively, and Stokes shifts of 3 and 5 nm for the Si(IV) and Zn(II) complexes, respectively, as it is typical for this type of compound (Figure 2).[42–45] Although the Zn(II)−Pcs show aggregation in protic solvents (methanol and water), as evidenced by the splitting and/or broadening of their *Q* absorption bands and significant decrease in the intensity of their emission bands and quantum yields, the Si(IV)−Pcs show intense and sharp *Q* bands and the highest fluorescence quantum yields in methanol solution. Pc aggregation in solution often results in broadening of the *Q* band absorptions and bathochromic and hypsochromic shifts.[46,47] Whereas only a few examples of J-type aggregates have been documented, for example protonation of a tetrasulfonated Zn(II)−Pc in aqueous acetonitrile caused a bathochromic shift of the *Q* band,[48] most of the aggregates are believed to be H-type, causing blue shifts and fluorescence quenching.[46,49–51] Although the octa-cationic Zn(II)−Pcs **10** and **11** exist in their monomeric forms in DMSO, showing sharp *Q* absorption bands at 677 nm (Figure 2a and b) and emission bands at 682 nm (Figure 2g and h), in aqueous media, they both form H-type aggregates as seen by the broadening and pronounced reduction in the intensity of their absorption and emission bands, along with reduction of their fluorescence quantum yields. Among all the Pcs evaluated in this study, Zn(II)−Pc **10** has the strongest tendency for aggregation in aqueous media, and as a result, it shows fluorescence quantum yields in water about one order of magnitude lower than all other cationic Pcs **11**−**15**. The presence of the eight tri(ethylene glycol) chains on Zn(II)−Pc **11** significantly decreases its tendency for aggregation in aqueous media compared with Zn(II)−Pc **10** bearing eight methyl groups, and as a result, Pc **11**'s *Q* absorption band follows the Lambert–Beer Law (see Figure S6 in the Supporting Information). However, the most efficient structural feature for minimizing aggregation of these cationic macrocycles is the presence of a centrally chelated silicon ion and associated bulky axial ligands. All Si(IV)−phthalocyanines **12**−**15** were found to exist mainly as monomers in both DMSO and aqueous solutions, showing similar intense and sharp *Q* band absorptions (Figure 2c−f) that strictly follow the Lambert–Beer Law (see Figures S7–S10 in the Supporting Information) and similarly intense emission bands (Figure 2i−l and Figures S7–S10 in the Supporting Information) in both media.

The singlet oxygen quantum yields for Pcs **11**−**15** were determined in DMSO as previously reported,[38] in the range 0.09–0.15, as shown in Table S5 of the Supporting Information. These values are characteristic for this type of Pc;[32,38] Si(IV)−Pc **13** was found to have the highest singlet oxygen quantum yield whereas Si(IV)−Pc **15** bearing eight short PEG chains had the lowest. It is possible that the singlet oxygen is inactivated by the PEG chains, as it has been previously observed.[52,53] Pc **13**,

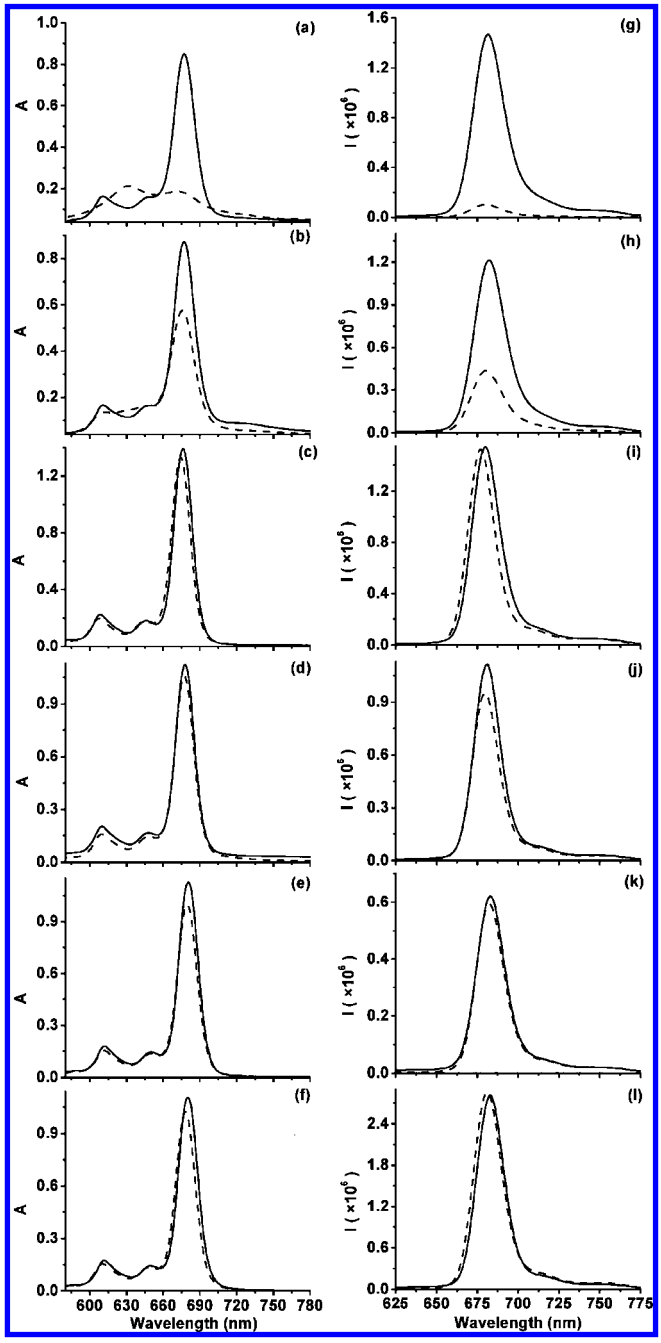

Figure 2. (a−f) Absorption spectra of Pcs **10**–**15** at 5 μM in DMSO (solid line) and in phosphate buffer (100 mM, pH 7.4) (dashed line). (g−l) Emission spectra of Pcs **10**–**15** at 80 nM in DMSO (solid line) and in phosphate buffer (100 mM, pH 7.4) (dashed line).

the most hydrophobic of all the Si(IV)−Pcs synthesized, shows the highest quantum yields in DMSO.

3. Cell Culture Studies. 3.1. Time-Dependent Cellular Uptake. The results obtained for the time-dependent uptake of Pcs **11**−**15** at a concentration of 10 μM in human HEp2 cells are shown in Figure 3. The cellular properties of Zn(II)−Pc **10** were not investigated due to its poor solubility in aqueous solution. All Pcs showed similar uptake kinetics with rapid accumulation at short time points and reaching a plateau after about 2 h. Zn(II)−Pc **11** bearing eight tri(ethylene glycol) groups was found to have the highest uptake at all time points investigated of this series of cationic Pcs, whereas Si(IV)−Pc **15** had the lowest. This result indicates that Zn(II)−Pc **11** probably has the most favorable amphiphilicity for crossing the

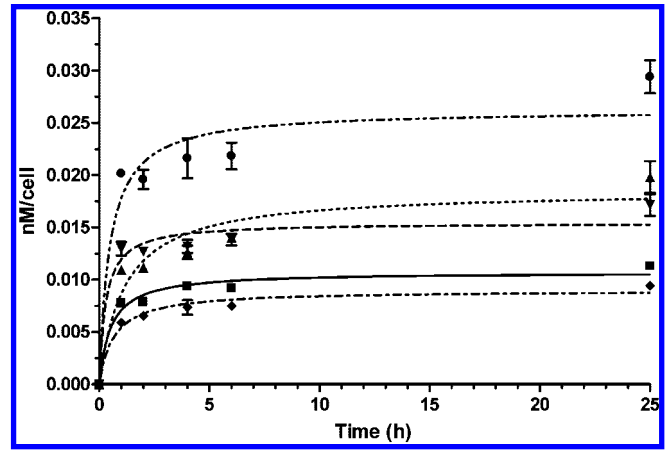

Figure 3. Time-dependent uptake of Pc **11** (circles, dot−dot−dash), Pc **12** (squares, full line), Pc **13** (triangles, dotted line), Pc **14** (inverted triangles, dashed line), and Pc **15** (diamonds, dot−dash) at 10 μM by HEp2 cells.

HEp2 cells plasma membranes. Although PEG-containing molecules generally have enhanced water solubility, serum life, and tumor accumulation,[54,55] we have recently shown that the accumulation of porphyrins within HEp2 cells depends on the number of PEG-substituents at the macrocycle periphery.[56] *meso*-Tetraphenylporphyrins containing three or four low molecular weight PEG chains accumulated to a lower extent within HEp2 cells than those containing one or two PEGs.

The cellular uptake of phthalocyanines and related macrocycles is known to depend on their hydrophobic character, overall charge, and charge distribution.[57,58] On the basis of the octanol/aqueous buffer (pH 7.4) distribution coefficients[39] of this series of Pcs (see Table S6 of the Supporting Information), the hydrophobic character of this series of Pcs, and the extent of their cellular uptake, increases in the order **15** < **12** < **14** < **13** < **11**. Si(IV)−Pc **13** bearing two triisopropylsiloxy axial groups is the most hydrophobic among the silicon Pcs whereas Si(IV)−Pc **15** bearing eight short PEG chains is the most hydrophilic of this series of Pcs and consequently the least taken up by cells.

3.2. Cytotoxicity. The dark-toxicity of Pcs **11**−**15** was evaluated in human HEp2 cells exposed to increasing concentrations of each Pc up to 100 μM, and the results are shown in Figure 4. Only Zn(II)−Pc **11**, the most accumulated within cells, showed measurable dark toxicity with an estimated $IC_{50} \sim 85$ μM. All Si(IV)−Pcs were found to be nontoxic to HEp2 cells in the dark up to 100 μM concentrations. However, upon exposure to a low light dose (1 J cm^{-2}), all Pcs were highly toxic to HEp2 cells, as shown in Figure 5. Pcs **11**, **12**, and **14** were the most phototoxic ($IC_{50} \sim 2.2$ μM), followed by Si(IV)−Pc **15** ($IC_{50} \sim 3.7$ μM) and Si(IV)−Pc **13** ($IC_{50} \sim 7.2$ μM). These results show, as previously observed,[59] that the phototoxicity of Pcs depends not only on the extent of their uptake into cells but also on their intracellular distribution and ability for generating reactive oxygen species (ROS). Si(IV)−Pcs **12** and **14** showed the highest quantum yields in aqueous media at pH 7.4 (vide supra) and might have higher ability for producing ROS. Although Pc **13** exhibited the highest singlet oxygen quantum yield in DMSO of this series of Pcs, its phototoxicity was lower than that of the other Si(IV)−Pcs, possibly due to its higher hydrophobicity compared with the other Si−Pcs and consequently its tendency for aggregation in aqueous solution. Pc **13** was also found to have the highest fluorescence quantum yield in DMSO but the lowest of all

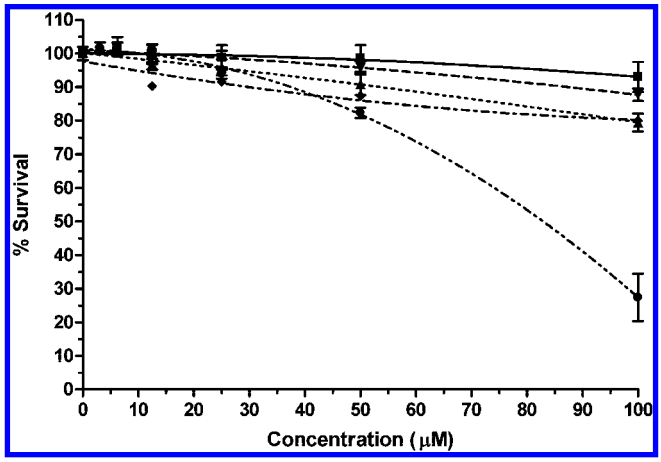

Figure 4. Dark toxicity of Pc **11** (circles, dot−dot−dash), Pc **12** (squares, full line), Pc **13** (triangles, dotted line), Pc **14** (inverted triangles, dashed line), and Pc **15** (diamonds, dot−dash) toward HEp2 cells using the Cell Titer Blue assay.

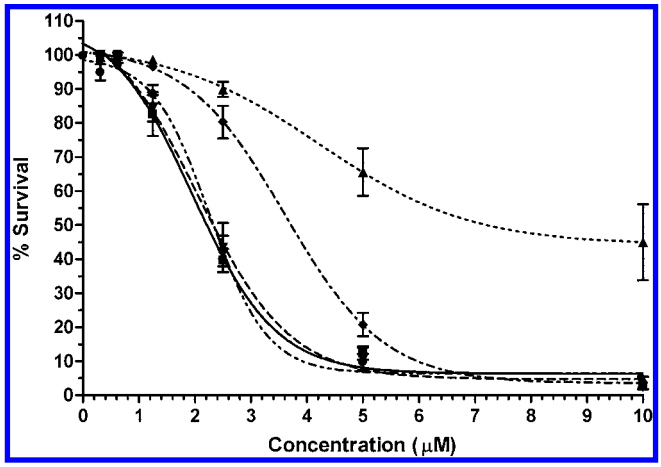

Figure 5. Phototoxicity of Pc **11** (circles, dot−dot−dash), Pc **12** (squares, full line), Pc **13** (triangles, dotted line), Pc **14** (inverted triangles, dashed line), and Pc **15** (diamonds, dot−dash) toward HEp2 cells using 1 J cm^{-2} light dose.

Si(IV)−Pcs in water at pH 7.0 (Table 1). It has been previously reported that although a dichlorinated Pc exhibited a higher singlet oxygen quantum yield in DMSO than the corresponding nonchlorinated Pc, its ability for generating ROS was lower probably as a consequence of its higher hydrophobicity and tendency for aggregation.[32] On the other hand, the high phototoxicity of Zn(II)−Pc **11** might result from both its high cellular uptake and ability for generating ROS, including singlet oxygen. Our results show that the nature of the axial ligands on Si(IV)−Pcs determines not only their photophysical properties but also their aggregation behavior and phototoxicity.

3.3. Intracellular Localization. The preferential sites of subcellular localization of this series of cationic Pcs were evaluated by fluorescence microscopy, upon exposure of HEp2 cells to 10 μM Pc concentrations overnight. Figure 6 shows the fluorescent pattern observed for Si(IV)−Pc **15** and its overlay with the organelle specific fluorescent probes BODIPY Ceramide (Golgi), LysoSensor Green (lysosomes), MitoTracker Green (mitochondria), and $DiOC_6$ (ER). Additional subcellular images for Pcs **11**−**14** are provided in the Supporting Information, Figures S27–S30. All Pcs were found to localize mainly within vesicles, which correlated well with the cell lysosomes (Figure 6f and Supporting Information). We did not observe any Pc relocalization during irradiation, as previously detected

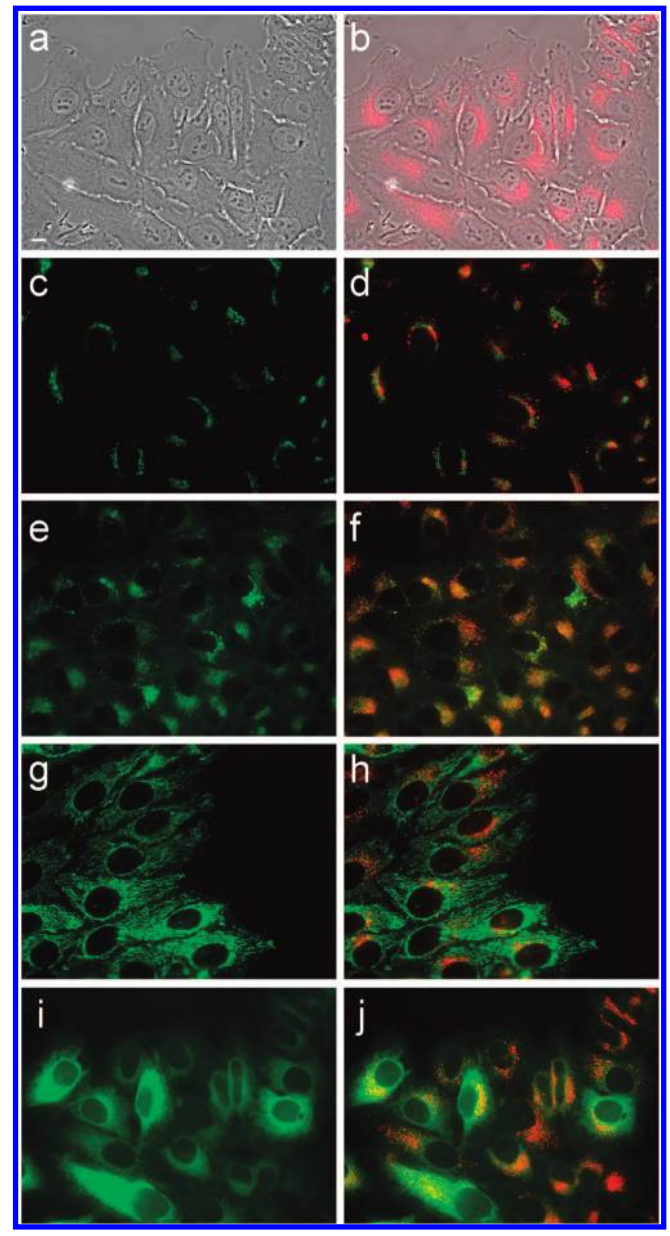

Figure 6. Subcellular localization of Si(IV)−Pc **15** in HEp2 cells at 10 μM for 24 h. (a) Phase contrast. (b) Overlay of **15** fluorescence and phase contrast. (c) BODIPY Ceramide fluorescence. (e) LysoSensor Green fluorescence. (g) MitoTracker Green fluorescence. (i) $DiOC_6$ fluorescence. (d, f, h, and j) Overlays of organelle tracers with **15** fluorescence: scale bar 10 μm.

for carboxylate-substituted Pcs.[19] In agreement with our results, a series of porphyrin- and Pc-peptide conjugates bearing multiple cationic residues, and of PEG-substituted porphyrins, were found to localize preferentially within the cell lysosomes.[42,56,60] Preferential lysosome localization has also been reported for several cationic porphyrins (e.g., see refs 61 and 62) probably as a result of an endocytic mechanism of cellular uptake. The lysosomes are considered important targets for the PDT-induced initiation of apoptosis.[63]

Conclusions

A series of cationic pyridyloxy Pcs (**11**−**15**) bearing either Zn(II) or Si(IV) coordinated metal ions and methyl or short PEG groups on the pyridyls, was synthesized. The Si(IV)−Pcs bearing two bulky axial ligands exist mainly as monomers in both organic and aqueous solutions and show higher fluores-

cence quantum yields in solution than the Zn(II)−Pcs. Both Zn(II)−Pcs form aggregates in aqueous media, in particular Pc **10** bearing eight *N*-methyl groups; the presence of eight short PEGs increases the solubility of the Pc macrocycle in protic solvents, but a centrally chelated silicon ion and associated bulky axial ligands are more efficient in minimizing Pc aggregation. This series of Pcs exhibited singlet oxygen quantum yields in DMSO in the range 0.09–0.15, and their in vitro properties depended on their hydrophobic character. The most hydrophobic Pc tested (**11**) accumulated the most within HEp2 cells and was highly phototoxic ($IC_{50} = 2.2\ \mu M$ at a 1 J cm^{-2} light dose). Among the Si(IV)−Pcs, the amphiphilic Pcs **12** and **14** were also highly phototoxic ($IC_{50} = 2.2\ \mu M$ at a 1 J cm^{-2} light dose). Despite their octa-cationic nature, all Pcs localized subcellularly preferentially within the lysosomes.

Acknowledgment. The authors thank Dr. Irina Nesterova for assistance with the photophysical studies. This work was supported by the National Science Foundation, grant number CHE-304833.

Supporting Information Available: Additional spectral data, octanol/aqueous buffer distribution coefficients, ^{1}H NMR, and fluorescence microscopy images for Pcs **11**−**14**. This material is available free of charge via Internet at http://pubs.acs.org.

References

(1) Allen, C. M.; Sharman, W. M.; Van Lier, J. E. Current status of phthalocyanines in the photodynamic therapy of cancer. *J. Porphyrins Phthalocyanines* **2001**, *5*, 161–169.

(2) Dougherty, T. J.; Gomer, C. J.; Henderson, B. W.; Jori, G.; Kessel, D.; Korbelik, M.; Moan, J.; Peng, Q. Photodynamic therapy. *J. Natl. Cancer Inst.* **1998**, *90*, 889–905.

(3) Hahn, S. M.; Glatstein, E. The emergence of photodynamic therapy as a major modality in cancer treatment. *Rev. Contemp. Pharm.* **1999**, *10*, 69–74.

(4) Pandey, R. K. Recent advances in photodynamic therapy. *J. Porphyrins Phthalocyanines* **2000**, *4*, 368–373.

(5) Brown, S. B.; Brown, E. A.; Walker, I. The present and future role of photodynamic therapy in cancer treatment. *Lancet Oncol.* **2004**, *5*, 497–508.

(6) Garcia-Zuazaga, J.; Cooper, K. D.; Baron, E. D. Photodynamic therapy in dermatology: current concepts in the treatment of skin cancer. *Expert Rev. Anticancer Ther.* **2005**, *5*, 791–800.

(7) Huang, Z. A review of progress in clinical photodynamic therapy. *Tech. Cancer Res. Treat.* **2005**, *4*, 283–293.

(8) Sharman, W. M.; Allen, C. M.; van Lier, J. E. Photodynamic therapeutics: basic principles and clinical applications. *Drug Discovery Today* **1999**, *4*, 507–517.

(9) Berg, K.; Selbo, P. K.; Weyergang, A.; Dietze, A.; Prasmickaite, L.; Bonsted, A.; Engesaeter, B. O.; Angell-Petersen, E.; Warloe, T.; Frandsen, N.; Hogset, A. Porphyrin-related photosensitizers for cancer imaging and therapeutic applications. *J. Microsc.* **2005**, *218*, 133–147.

(10) Allison, R. R.; Downie, G. H.; Cuenca, R.; Hu, X. H.; Childs, C. J.; Sibata, C. H. Photosensitizers in clinicla PDT. *Photodiagn. Photodyn. Ther.* **2004**, *1*, 27–42.

(11) Detty, M. R.; Gibson, S. L.; Wagner, S. J. Current clinical and preclinical photosensitizers for use in photodynamic therapy. *J. Med. Chem.* **2004**, *47*, 3897–3915.

(12) Brown, S.; Brown, E. A.; Walker, I. The present and future role of photodynamic therapy in cancer treatment. *Lancet Oncol.* **2004**, *5*, 497–508.

(13) Huang, Z. A review of progress in clinical photodynamic therapy. *Tech. Cancer Res. Treat.* **2005**, *4*, 283–293.

(14) Stillman, M. J.; Nyokong, T. Absorption and magnetic circular dichroism spectral properties of phthalocyanine part 1: Complexes of the dianion Pc (−2). *Phthalocyanine—Properties and Applications*; Leznoff, C. C., Lever, A. B. P., Eds.; VCH Publishers: Germany, 1989.

(15) Mckeown, N. B. *Phthalocyanine Materials—Synthesis, Structure and Function*; Cambridge University Press: UK, 1998.

(16) DeRosa, M. C.; Crutchley, R. J. Photosensitized singlet oxygen and its applications. *Coord. Chem. Rev.* **2002**, *233*, 351–371.

(17) (a) Huang, J. D.; Wang, S. Q.; Lo, P. C.; Fong, W. P.; Ko, W. H.; Ng, D. K. P. Halogenated silicon(IV) phthalocyanines with axial poly(ethylene glycol) chains. Synthesis, spectroscopic properties, complexation with bovine serum albumin and in vitro photodynamic activities. *New J. Chem.* **2004**, *28*, 348–354. (b) Lo, P. C.; Huang, J. D.; Cheng, D. Y. Y.; Chan, E. Y. M.; Fong, W. P.; Ko, W. H.; Ng, D. K. P. New amphiphilic silicon(IV) phthalocyanines as efficient photosensitizers for photodynamic therapy: Synthesis, photophysical properties, and in vitro photodynamic activities. *Chem.—Eur. J.* **2004**, *10*, 4831–4838.

(18) (a) Lee, P. P. S.; Lo, P. C.; Chan, E. Y. M.; Fong, W. P.; Ko, W. H.; Ng, D. K. P. Synthesis and in vitro photodynamic activity of novel galactose-containing phthalocyanines. *Tetrahedron Lett.* **2005**, *46*, 1551–1554. (b) Huang, J. D.; Lo, P. C.; Chen, Y. M.; Lai, J. C.; Fong, W. P.; Ng, D. K. P. Preparation and in vitro photodynamic activity of novel silicon(IV) phthalocyanines conjugated to serum albumins. *J. Inorg. Biochem.* **2006**, *100*, 946–951.

(19) Liu, W.; Jensen, T. J.; Fronczek, F. R.; Hammer, R. P.; Smith, K. M.; Vicente, M. G. H. Synthesis and cellular studies of nonaggregated water-soluble phthalocyanines. *J. Med. Chem.* **2005**, *48*, 1033–1041.

(20) Yang, Y.-C.; Ward, J. R.; Seiders, R. P. Dimerization of cobalt(II) tetrasulfonated phthalocyanine in water and aqueous alcoholic solutions. *Inorg. Chem.* **1985**, *24*, 1765–176.

(21) Oleinick, N. L.; Antunez, A. R.; Clay, M. E.; Rihter, B. D.; Kenney, M. E. New phthalocyanine photosensitizers for photodynamic therapy. *Photochem. Photobiol.* **1993**, *57*, 242–247.

(22) He, J.; Larkin, H. E.; Li, Y. S.; Rihter, B. D.; Zaidi, S. I. A.; Rodgers, M. A. J.; Mukhtar, H.; Kenney, M. E.; Oleinick, N. L. The synthesis, photophysical and photobiological properties and in vitro structure-activity relationships of a set of silicon phthalocyanine PDT photosensitizers. *Photochem. Photobiol.* **1997**, *65*, 581–586.

(23) (a) Lee, P. P. S.; Ngai, T.; Huang, J. D.; Wu, C.; Fong, W. P.; Ng, D. K. P. Synthesis, characterization, biodegradation, and in vitro photodynamic activities of silicon(IV) phthalocyanines conjugated axially with poly(epsilon-caprolactone). *Macromolecules* **2003**, *36*, 7527–7533. (b) Lee, P. P. S.; Ngai, T.; Cheng, Y.; Chi, W.; Ng, D. K. P. Synthesis, characterization, and degradation of silicon(IV) phthalocyanines conjugated axially with poly(sebacic anhydride). *J. Polym. Sci. Part A: Polym. Chem.* **2005**, *43*, 837–843.

(24) Zhu, Y. J.; Huang, J. D.; Jiang, X. J.; Sun, J. C. Novel silicon phthalocyanines axially modified by morpholine: Synthesis, complexation with serum protein and in vitro photodynamic activity. *Inorg. Chem. Commun.* **2006**, *9*, 473–477.

(25) Sonoda, M.; Krishna, C. M.; Riesz, P. The role of singlet oxygen in the photohemolysis of red-blood-cells sensitized by phthalocyanine sulfonates. *Photochem. Photobiol.* **1987**, *46*, 625–631.

(26) (a) Ball, D. J.; Wood, S. R.; Vernon, D. I.; Griffiths, J.; Dubbelman, T. M. A. R.; Brown, S. B. The characterisation of three substituted zinc phthalocyanines of differing charge for use in photodynamic therapy. A comparative study of their aggregation and photosensitising ability in relation to mTHPC and polyhaematoporphyrin. *J. Photochem. Photobiol. B: Biol.* **1998**, *45*, 28–35. (b) Ball, D. J.; Mayhew, S.; Wood, S. R.; Griffiths, J.; Vernon, D. I.; Brown, S. B. A comparative study of the cellular uptake and photodynamic efficacy of three novel zinc phthalocyanines of differing charge. *Photochem. Photobiol.* **1999**, *69*, 390–396.

(27) Wohrle, D.; Iskander, N.; Graschew, G.; Sinn, H.; Friedrich, E. A.; Maierborst, W.; Stern, J.; Schlag, P. Synthesis of positively charged phthalocyanines and their activity in the photodynamic therapy of cancer cells. *Photochem. Photobiol.* **1990**, *51*, 351–356.

(28) Michelsen, U.; Kliesch, H.; Schnurpfeil, G.; Sobbi, A. K.; Wohrle, D. Unsymmetrically substituted benzonaphthoporphyrazines: A new class of cationic photosensitizers for the photodynamic therapy of cancer. *Photochem. Photobiol.* **1996**, *64*, 694–701.

(29) Sobbi, A. K.; Wohrle, D.; Schlettwein, D. Photochemical stability of various porphyrins in solution and as thin-film electrodes. *J. Chem. Soc., Perkin Trans. 2* **1993**, 481–488.

(30) (a) Minnock, A.; Vernon, D. I.; Schofield, J.; Griffiths, J.; Parish, J. H.; Brown, S. B. Photoinactivation of bacteria. Use of a cationic water-soluble zinc phthalocyanine to photoinactivate both gram-negative and gram-positive bacteria. *J. Photochem. Photobiol. B: Biol.* **1996**, *32*, 159–164. (b) Minnock, A.; Vernon, D. I.; Schofield, J.; Griffiths, J.; Parish, J. H.; Brown, S. B. Mechanism of uptake of a cationic water-soluble pyridinium zinc phthalocyanine across the outer membrane of Escherichia coli. *Antimicrob. Agents Chemother.* **2000**, *44*, 522–527.

(31) Scalise, I.; Durantini, E. N. Synthesis, properties, and photodynamic inactivation of Escherichia coli using a cationic and a noncharged Zn(II) pyridyloxyphthalocyanine derivatives. *Bioorg. Med. Chem.* **2005**, *13*, 3037–45.

(32) Lo, P. C.; Chan, C. M. H.; Liu, J. Y.; Fong, W. P.; Ng, D. K. P. Highly photocytotoxic glucosylated Silicon(IV) phthalocyanines. Effects of peripheral chloro substitution on the photophysical and photodynamic properties. *J. Med. Chem.* **2007**, *50*, 2100–2107.

(33) Hofman, J. W.; Zeeland, F. V.; Turker, S.; Talsma, H.; Lambrechts, S. A.; Sakharov, D. V.; Hennink, W. E.; Nostrum, C. F. Peripheral and axial substitution of phthalocyanines with solketal groups: Synthesis and in vitro evaluation for photodynamic therapy. *J. Med. Chem.* **2007**, *50*, 1485–1494.
(34) Schultz, R. A.; White, B. D.; Dishong, D. M.; Arnold, K. A.; Gokel, G. W. 12-Membered, 15-membered, and 18-membered-ring nitrogen-pivot lariat ethers - syntheses, properties, and sodium and ammonium cation binding-properties. *J. Am. Chem. Soc.* **1985**, *107*, 6659–6668.
(35) Fery-Forgues, S.; Lavabre, D. Are fluorescence quantum yields so tricky to measure? A demonstration using familiar stationery products. *J. Chem. Educ.* **1999**, *76*, 1260–1264.
(36) Olmsted, J. Calorimetric determinations of absolute fluorescence quantum yields. *J. Phys. Chem.* **1979**, *83*, 2581–2584.
(37) Lakowicz, J. R. *Principles of Fluorescence Spectroscopy*, 2nd ed.; Kluwer Academic/Plenum Publisher; New York, 1999; pp 52f.
(38) Maree, M. D.; Kuznetsova, N.; Nyokong, T. Silicon octaphenoxyphthalocyanines: photostability and singlet oxygen quantum yields. *J. Photochem. Photobiol. A: Chem.* **2001**, *140*, 117–125.
(39) Vicente, M. G. H.; Edwards, B. F.; Shetty, S. J.; Hou, Y.; Boggan, J. E. Synthesis and preliminary biological studies of four tetra(*nido*-carboranylmethylphenyl)porphyrins. *Bioorg. Med. Chem.* **2002**, *10*, 481–492.
(40) Wöhrle, D.; Eskes, M.; Shigehara, K.; Yamada, A. A Simple Synthesis of 4,5-Disubstituted 1,2-Dicyanobenzenes and 2,3,9,10,16,17,23,24-Octasubstituted Phthalocyanines. *Synthesis-Stuttgart* **1993**, 194–196.
(41) De Filippis, M. P.; Dei, D.; Fantetti, L.; Roncucci, G. Synthesis of a new water-soluble octa-cationic phthalocyanine derivative for PDT. *Tetrahedron Lett.* **2000**, *41*, 9143–9147.
(42) Sibrian-Vazquez, M.; Ortiz, J.; Nesterova, I. V.; Fernandez-Lazaro, F.; Sastre-Santos, A.; Soper, S. A.; Vicente, M. G. H. Synthesis and properties of cell-targeted Zn(II)-phthalocyanine-peptide conjugates. *Bioconjugate Chem.* **2007**, *18*, 410–420.
(43) Darwent, J. R.; Douglas, P.; Harriman, A.; Porter, G.; Richoux, M. C. Metal Phthalocyanines and Porphyrins as Photosensitizers for Reduction of Water to Hydrogen. *Coord. Chem. Rev.* **1982**, *44*, 83–126.
(44) Ali, H.; van Lier, J. E. Metal complexes as photo- and radiosensitizers. *Chem. Rev.* **1999**, *99*, 2379–2450.
(45) Barker, C. A.; Findlay, K. S.; Bettington, S.; Batsanov, A. S.; Perepichka, I. F.; Bryce, M. R.; Beeby, A. Synthesis of new axially-disubstituted silicon-phthalocyanine derivatives: optical and structural characterisation. *Tetrahedron* **2006**, *62*, 9433–9439.
(46) Farren, C.; FitzGerald, S.; Beeby, A.; Bryce, M. R. The first genuine observation of fluorescent mononuclear phthalocyanine aggregates. *Chem. Commun.* **2002**, 572–573.
(47) Ma, C. Y.; Ye, K. Q.; Yu, S. K.; Du, G. T.; Zhao, Y. F.; Cong, F. D.; Chang, Y. C.; Jiang, W. H.; Cheng, C. H.; Fan, Z. Q.; Yu, H. F.; Li, W. C. Synthesis and hypochromic effect of phthalocyanines and metal phthalocyanines. *Dyes Pigm.* **2007**, *74*, 141–147.
(48) Beeby, A.; FitzGerald, S.; Stanley, C. F. Protonation of tetrasulfonated zinc phthalocyanine in aqueous acetonitrile solution. *Photochem. Photobiol.* **2001**, *74*, 566–569.
(49) Howe, L.; Zhang, J. Z. Ultrafast studies of excited-state dynamics of phthalocyanine and zinc phthalocyanine tetrasulfonate in solution. *J. Phys. Chem. A* **1997**, *101*, 3207–3213.
(50) Dhami, S.; Demello, A. J.; Rumbles, G.; Bishop, S. M.; Phillips, D.; Beeby, A. Phthalocyanine fluorescence at high concentration - dimers or reabsorption effect. *Photochem. Photobiol.* **1995**, *61*, 341–346.
(51) Kameyama, K.; Morisue, M.; Satake, A.; Kobuke, Y. Highly fluorescent self-coordinated phthalocyanine dimers. *Angew. Chem., Int. Ed.* **2005**, *44*, 4763–4766.
(52) Kanofsky, J. R. Quenching of singlet oxygen by human plasma. *Photochem. Photobiol.* **1990**, *51*, 299–303.
(53) Reuther, T.; Kubler, A. C.; Zillmann, U.; Flechtenmacher, C.; Sinn, H. Comparison of the in vivo efficiency of photofrin II-, mTHPC-, mTHPC-PEG- and mTHPCnPEG-mediated PDT in a human xenografted head and neck carcinoma. *Lasers Surg. Med.* **2001**, *29*, 314–322.
(54) (a) Greenwald, R. B. PEG drugs: an overview. *J. Controlled Release* **2001**, *74*, 159–171. (b) Greenwald, R. B.; Choe, Y. H.; McGuire, J.; Conover, C. D. Effective drug delivery by PEGylated drug conjugates. *Adv. Drug Delivery Rev.* **2003**, *55*, 217–250.
(55) Hamblin, M. R.; Miller, J. L.; Rizvi, I.; Loew, H. G.; Hasan, T. Pegylation of charged polymer-photosensitizer conjugates: effects on photodynamic therapy. *Br. J. Cancer* **2003**, *89*, 937–943.
(56) Sibrian-Vazquez, M.; Jensen, T. J.; Vicente, M. G. H. Synthesis and Cellular Studies of PEG-functionalized meso-Tetraphenylporphyrins. *J. Photochem. Photobiol. B: Biol.* **2007**, *86*, 9–21.
(57) (a) Berg, K.; Bommer, J. C.; Moan, J. Evaluation of sulfonated aluminum phthalocyanines for use in photochemotherapy - Cellular uptake studies. *Cancer Lett.* **1989**, *44*, 7–15. (b) Berg, K.; Bommer, J. C.; Moan, J. Evaluation of sulfonated aluminum phthalocyanines for use in photochemotherapy - a study on the relative efficiencies of photoinactivation. *Photochem. Photobiol.* **1989**, *49*, 587–594.
(58) Hammer, N. D.; Lee, S.; Vesper, B. J.; Elseth, K. M.; Hoffman, B. M.; Barrett, A. G. M.; Radosevich, J. A. Charge dependence of cellular uptake and selective antitumor activity of porphyrazines. *J. Med. Chem.* **2005**, *48*, 8125–8133.
(59) Cauchon, N.; Tian, H. J.; Langlois, J.; La Madeleine, C.; Martin, S.; All, H.; Hunting, D.; van Lier, J. E. Structure-photodynamic activity relationships of substituted zinc trisulfophthalocyanines. *Bioconjugate Chem.* **2005**, *16*, 80–89.
(60) (a) Sibrian-Vazquez, M.; Jensen, T. J.; Fronczek, F. R.; Hammer, R. P.; Vicente, M. G. H. Synthesis and characterization of positively charged porphyrin-peptide conjugates. *Bioconjugate Chem.* **2005**, *16*, 852–863. (b) Sibrian-Vazquez, M.; Jensen, T. J.; Hammer, R. P.; Vicente, M. G. H. Peptide-mediated cell transport of water soluble porphyrin conjugates. *J. Med. Chem.* **2006**, *49*, 1364–1372.
(61) Kessel, D.; Luguya, R.; Vicente, M. G. H. Localization and photodynamic efficacy of two cationic porphyrins varying in charge distribution. *Photochem. Photobiol.* **2003**, *78*, 431–435.
(62) Ricchelli, F.; Franchi, L.; Miotto, G.; Borsetto, L.; Gobbo, S.; Nikolov, P.; Bommer, J. C.; Reddi, E. Meso-substituted tetra-cationic porphyrins photosensitize the death of human fibrosarcoma cells via lysosomal targeting. *Int. J. Biochem. Cell Biol.* **2005**, *37*, 306–19.
(63) Tardy, C.; Codogno, P.; Autefage, H.; Levade, T.; Andrieu-Abadie, N. Lysosomes and lysosomal proteins in cancer cell death (new players of an old struggle). *Biochim. Biophys. Acta* **2006**, *1765*, 101–125.

JM070781F